The target velocity integration function for saccades

Peter J. Etchells Department of Experimental Psychology, University of Bristol, Bristol, UK

Christopher P. Benton Department of Experimental Psychology, University of Bristol, Bristol, UK

Casimir J. H. Ludwig Department of Experimental Psychology, University of Bristol, Bristol, UK

Iain D. Gilchrist Department of Experimental Psychology, University of Bristol, Bristol, UK

Interacting with a dynamic environment calls for close coordination between the timing and direction of motor behaviors. Accurate motor behavior requires the system to predict where the target for action will be, both when action planning is complete and when the action is executed. In the current study, we investigate the time course of velocity information accrual in the period leading up to a saccade toward a moving object. In two experiments, observers were asked to generate saccades to one of two moving targets. Experiment 1 looks at the accuracy of saccades to targets that have trial-by-trial variations in velocity. We show that the pattern of errors in saccade landing position is best explained by proposing that trial-by-trial target velocity is taken into account in saccade planning. In Experiment 2, target velocity stepped up or down after a variable interval after the movement cue. The extent to which the movement endpoint reflects pre- or post-step velocity can be used to identify the temporal velocity integration window; we show that the system takes a temporally blurred snapshot of target velocity centered ~200 ms before saccade onset. This estimate is used to generate a dynamically updated prediction of the target's likely future location.

Keywords: eye movement, saccade, prediction, velocity, motion

Citation: Etchells, P. J., Benton, C. P., Ludwig, C. J. H., & Gilchrist, I. D. (2010). The target velocity integration function for saccades. *Journal of Vision, 10*(6):7, 1–14, http://www.journalofvision.org/content/10/6/7, doi:10.1167/10.6.7.

Introduction

The visual environment contains objects with a diverse range of movement characteristics. Generating appropriately timed saccadic and other motor responses to such objects is essential in order to successfully interact with the environment. While we know a great deal about the neural processes underlying saccade target selection and generation (e.g., Schall, 1999; Schiller & Tehovnik, 2005), much of this work is based on eye movements in a static world. A more complete understanding of saccade planning should include knowledge of how the system deals with visual signals in a dynamic world.

Part of the potential problem for any motor response is that there is a neuronal delay between the decision to move and the actual movement execution (Kerzel & Gegenfurtner, 2003). For saccades, this delay includes the so-called saccadic dead time, the period directly preceding saccade onset during which new visual information can no longer influence the movement endpoint (often estimated to be around 80 ms; Aslin & Shea, 1987; Becker & Jürgens, 1979; Caspi, Beutter, & Eckstein, 2004; Findlay & Harris, 1984).

Prediction also needs to take into account the actual saccade movement duration, which will be dependent upon the movement amplitude (Bahill & Stark, 1975). Essentially, for accurate saccade generation the system needs to predict where a moving target will be after the saccade has been completed.

There are two general ways in which this prediction could occur. The first, hereafter known as the "fixed offset" model, suggests that saccades could be generated based on retinal position error sampled at a point in time prior to saccade generation, to which a constant velocity-independent distance is applied (e.g., Heywood & Churcher, 1981). Alternatively, one could argue for a "velocity dependent" model. In this case, a representation of the target's velocity is extracted and used to generate a dynamically updated prediction of the target's likely future location.

Studies of non-human primates show that frontal eye field (FEF) neurons encode both target position and velocity alongside relevant saccade metrics (such as duration and amplitude) when planning a saccade to a smoothly moving target (Cassanello, Nihalani, & Ferrera, 2008). With respect

doi: 10.1167/10.6.7 Received December 8, 2009; published June 8, 2010 ISSN 1534-7362

to the smooth pursuit response in experiments involving the temporary occlusion of a moving target, non-human primate studies have shown that both target position (Barborica & Ferrera, 2004) and velocity (Barborica & Ferrera, 2003; Ilg & Thier, 2003) of the occluded target can be predicted by the oculomotor system. In particular, Barborica and Ferrera (2003) suggest that an internal estimate of target speed is used when programming predictive saccades and that this is correlated with neuronal activity in FEF. Target speed also appears to be a determining factor in the amplitude of the generated saccade (Eggert, Guan, Bayer, & Buttner, 2005) and the ability to generate accurate saccades to moving targets is abolished following lesions to area MT (Newsome, Wurtz, Dursteler, & Mikami, 1985), a brain area known to be involved in visual motion processing (Born & Bradley, 2005). Taken together, such studies provide a picture of the cortical basis for a velocity-dependent model.

The findings from human observers are less straightforward to interpret. While original evidence was cited in favor of velocity signals being used by the saccadic system (e.g., Robinson, 1973), it was later suggested (Heywood & Churcher, 1981) that saccadic behavior could be just as reasonably explained by a fixed-offset model that samples the retinal position error 100 ms prior to the saccade. On the basis of these findings, it was argued that speed-based prediction was not necessary in order to produce accurate saccade endpoints. Other studies have been inconclusive as to whether the saccadic system extracts velocity information in programming a primary orienting saccade to a moving target (Ron, Vieville, & Droulez, 1989).

A closely related issue has been addressed in the smooth pursuit literature, where the question is whether catch-up saccades take the target velocity into account (e.g., de Brouwer, Missal, Barnes, & Lefèvre, 2002; Gellman & Carl, 1991a; Keller & Johnsen, 1990; Kim, Thaker, Ross, & Medoff, 1997). These studies have highlighted an important role for "retinal slip", which includes the target velocity alongside other extra-retinal signals. It is argued that the saccadic system corrects the retinal position error and integrates the mean retinal slip over the saccade latency and duration in order to produce accurate landing positions. Under such conditions, the aim of the visual system is to coordinate smooth pursuit and saccadic movements in order to optimize visual behavior (Krauzlis, 2004; Krauzlis & Stone, 1999).

Given that there is evidence for shared visual processing between pursuit and saccadic systems (Liston & Krauzlis, 2005; Orban de Xivry & Lefèvre, 2007), and that one of the major inputs shared is target velocity (e.g., de Brouwer et al., 2002; Gellman & Carl, 1991a; Newsome et al., 1985), it is reasonable to suggest that velocity information should be available to the saccadic system for the purposes of making an initial orienting movement toward moving stimuli. However, the nature of the mechanism through which target velocity is incorporated into the metrics of the primary orienting saccade is unclear. Our aim was to shed light on this mechanism by identifying the period over which velocity information is extracted, if at all, prior to saccade generation.

General methods

Apparatus

Stimuli were displayed on a 21-inch, gamma-corrected CRT monitor (LaCie Electron Blue) running at 75 Hz. The monitor resolution was 1152 × 864 pixels. The screen subtended 36 deg of visual angle horizontally and 24 deg of visual angle vertically. A chin rest was used to stabilize the head position and was placed at a viewing distance of 57 cm from the screen. Eye movements were monitored using the EyelinkII (SR Research, Mississauga, Ontario, Canada), an infrared tracking system that uses the center of the pupil to sample eye position at 500 Hz and has a repeat calibration accuracy of ~0.3 deg. Observers viewed the display monocularly; eye dominance was determined with the hole-in-the-card technique (Seijas et al., 2007). Saccades were detected offline. For each data sample, the EyelinkII saccade parser algorithm (SR Research, Mississauga, Ontario, Canada) computes the instantaneous velocity and acceleration and compares these to threshold criteria for velocity and acceleration (30 deg/s and 8000 deg/s^2). If either was above threshold, the eye movement is classified as a saccade; a distance threshold of 0.1 deg was used to delay the onset of the saccade until the eye had moved significantly. At the end of the saccade, the signal was terminated if both the velocity and acceleration values were below the criterion thresholds, or if the inter-sample movement was below the distance threshold. This latter component of the algorithm was designed to prevent saccades being "stretched" as a result of erroneous endpoint localization (for a more complete description, see Stampe, 1993). Visual inspection of the eye traces confirmed that the parsing algorithm reliably identified the saccade start and endpoints.

The experimental software was programmed in Matlab using the Psychophysics Toolbox (Brainard, 1997) and Eyelink Toolbox extensions (Cornelissen, Peters, & Palmer, 2002). Both target and distractor stimuli were Gaussian patches. The pedestal peak luminance of the patterns was 36 cd/m^2. The target patch was signaled by increasing its peak luminance to 82 cd/m^2. The background luminance was 20.5 cd/m^2. The standard deviation of the patches was 0.32 deg of visual angle.

Experiment 1

The purpose of this first experiment was to first of all establish whether human observers are able to take target

velocity into account when generating primary orienting saccades to moving targets. The task required observers to fixate a central cross on a computer screen while two Gaussian patches traversed in a straight line, 6 deg of visual angle above and below the midline, horizontally across the screen at one of four speeds. Observers were instructed to wait until one of the patches stepped up in luminance, at which point they were told to generate, as quickly and as accurately as possible, a saccade to the brighter patch.

Methods

Observers

Five observers were recruited from students and staff of the University of Bristol, UK (4 males and 1 female, age range 18–40, mean age 25). Two observers had no previous experience with eye-tracking experiments. All observers had self-reported normal or corrected-to-normal vision. Data were collected over the course of two sessions, performed on different days. The study was approved by the local ethics committee.

Design and procedure

Observers performed 10 experimental blocks, each containing 96 trials. Each trial block was preceded by a nine-point calibration procedure in which observers were asked to fixate a black cross (measuring 0.3 deg × 0.3 deg) that appeared randomly at nine points on a 3 × 3 grid that subtended an area of 31 deg by 19 deg of visual angle on-screen. Observers were instructed to fixate a black fixation cross throughout each trial, until they detected a luminance change in the Gaussian patches, at which point they were required to make a saccade to the brighter patch (see Figure 1).

Within each block, the stimulus patches moved in 64 of the trials (half moving rightward and half leftward) and remained static in 16 trials. A further 8 trials consisted of static patches with no luminance change, and 8 moving trials with no luminance change (4 leftward and 4 rightward). In the movement trials, the patches could move at one of four constant speeds—6, 12, 18, and 24 deg/s.

Each trial began with the presentation of two equiluminant Gaussian patches 6 deg of visual angle above and below the horizontal midline of the screen. In trials in which the patches moved, the starting locations were determined such that the patches would be shown for at least 333 ms before the luminance change would occur. This was to ensure that observers had sufficient exposure to the stimulus speed to make an accurate speed judgment. After this time, we used a nonaging foreperiod to determine the moment of the luminance change. The mean of this exponential distribution was 128 ms, such that the change occurred at a variable point within a window covering approximately 6 deg of visual angle either side of fixation.

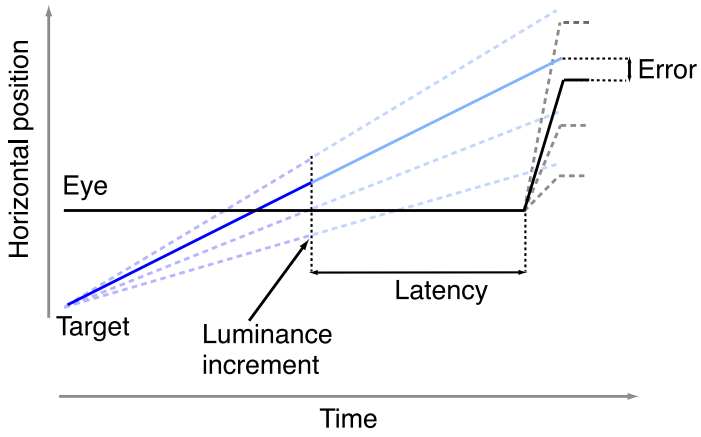

Figure 1. Time course of the target patch in a single trial in Experiment 1. Note that the non-target patch follows the same time course but is not subject to a luminance increment. Blue filled line denotes target moving at 18 deg/s. The target could also move at 6, 12, or 24 deg/s (denoted by the paler blue dashed lines). At a variable point during the trial, the luminance of one of the patches would increase (denoted by the light blue portion of the line), at which time we would begin recording saccade latency. After a primary orienting saccade was made, the error between saccade landing position and target position was recorded.

A nonaging foreperiod can be described as a foreperiod in which the probability of its immediate termination remains constant over time; the use of such a foreperiod results in the observer's expectation of when the luminance change would occur remaining constant throughout the trial (Oswal, Ogden, & Carpenter, 2007). This is desirable for the present series of experiments, because of the need to minimize anticipatory movements that are not guided by visual information in the stimulus.

After the luminance change, the patches would then carry on moving until they reached the opposite side of the screen and then disappear, ready for the next trial to begin. In the case of static trials, the patches would remain on-screen for a length of time that was variable from trial to trial that was equated with the amount of time they would have been visible had they been moving at each of the four speeds used in the motion trials.

Data analysis

Only data collected about the first saccade in each trial were considered for analysis. Further to this, the percentage of trials in which the inter-saccadic interval between first and second saccades was less than 100 ms constituted less than 5% for all five observers. Trials in which the amplitude of the first saccade was less than 4 deg were rejected. Data from trials in which no saccade was made (either due to participants not detecting a target change or there being no target change), as well as data from trials in which the patches remained static were not included in further analysis. Saccade endpoints were recorded, along

with the target location at saccade termination and saccade amplitude. The primary analysis concerned the horizontal component of each saccade.

Results

Figure 2 shows, for each observer, the observed error between saccade endpoint and the location of the target at saccade termination, as a function of the target velocity (blue dots). The linear regressions shown in the figure (solid lines) express the parameters of the fixed offset model necessary to predict that pattern of data. The reason for this is given as follows. If we assume that a position grab occurs some k seconds before saccade termination, and that a constant offset of d degrees is applied to the position grab to determine ideal landing position, then the error (ε) between target position and saccade landing position is

$$\varepsilon = d - kv_t, \quad (1)$$

where v_t is the speed of the target. The fixed offset model therefore predicts a linear relationship between v_t and ε with slope $-k$ and intercept d. Complete velocity dependence would show as a flat function aligned with the abscissa, or perhaps parallel to it in the presence of a general bias to under- or overshoot. The dashed lines in Figure 2 illustrate the predictions of a reasonable fixed-offset model in which the observer samples the "final" target position at 100 ms before saccade initiation (e.g., Becker & Jürgens, 1979; de Brouwer et al., 2002; Heywood & Churcher, 1981) and applies a fixed offset taking into account the average velocity experienced over the course of the experiment (15 deg/s) and the duration of the saccade (derived from the average duration for each observer across all trials).

The empirical data generally lie much closer to the zero-error axis, although there clearly is some systematic variation with target velocity. Examination of the regression slopes indicates that they range from about 20 ms to 55 ms with a mean of 39 ms. Given that the average saccade duration across all participants was 58 ms, a fixed offset interpretation of these data would imply that the final position grab would have to occur during the saccade itself and, of course, after saccadic dead time. These data, then, clearly support the notion that target velocity contributes to the metrics of the primary orienting saccade.

As stated above, if the saccadic system were able to take target position and velocity perfectly into account, then we would expect slopes of zero in the graphs shown in Figure 2. Clearly, this is not what we find. At higher target velocities, saccades tend increasingly to trail the target. One reason that this may occur is due to the fact that under laboratory conditions, saccades will often fall short of a desired target by an amount proportional to the amplitude. The amount of undershoot will be subject to a number of factors, such as general stimulus characteristics

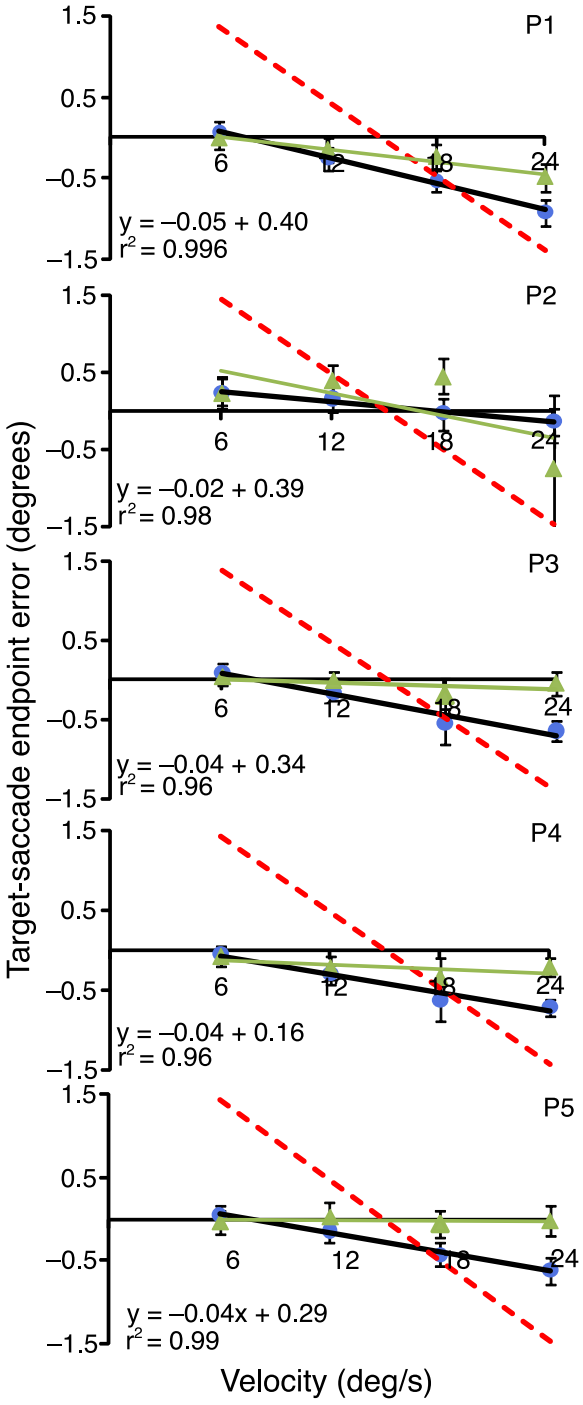

Figure 2. Error (in degrees) between where the saccade landed and where the target was when the saccade ended for each participant at each of the four velocities used in Experiment 1. Blue filled circles denote mean observed data (error bars show 95% confidence intervals). Black solid line denotes linear regression fit of observed data, with accompanying regression equation. Green filled triangles denote data corrected for an assumed saccadic undershoot of 10% of the desired amplitude. Red dashed line denotes a fixed-offset model prediction. For the latter, we assume that the saccadic system samples target position 100 ms prior to saccade generation and is adapted to give an accurate response to the average speed presented (15 deg/s).

and saccade requirements (Becker, 1989; Harris, 1994). Within the context of the current experiment, the particular factor of interest is target velocity—while saccade latency did not depend on the velocity (a repeated measures ANOVA showed no significant differences between the latencies for each of the velocities, $p = 0.48$), it is clear that amplitude did. As such, it is likely that saccades to the faster targets were larger in amplitude because participants are less likely to "catch" the moving target when it was near the center of the screen. If so, then the corresponding undershoot will also tend to be larger.

In order to test this, we assumed that this undershoot corresponded to 10% of the intended amplitude. This proportion corresponds to the average undershoot reported in experiments concerning saccades made to peripheral targets with abrupt onsets (Harris, 1994). We then used this to calculate the intended amplitude and, in turn, the resulting horizontal component of the saccade that would have been generated. In other words, we ask what the pattern of results would be like if we corrected for a 10% undershoot; this is shown by the green triangles in Figure 2. Clearly, correcting for this undershoot results in regression functions with slopes closer to zero than those for the raw saccades. The downward slopes found in our data (see Figure 2, blue dots) may therefore reasonably be accounted for by proportional undershoot. However, proportional undershoot cannot account for the mismatch between our data and the fixed-offset model. In fact, quite the opposite; correcting for proportional undershoot results in a decrease in slope. Our data therefore suggest that the human saccadic system does take an estimate of target velocity into account. We now turn toward the nature of this velocity estimation process.

Experiment 2

The purpose of this experiment was to investigate how observers estimate the target velocity to adjust their movements. Specifically, we sought to identify the period over which target velocity is integrated. Similar to Experiment 1, the task involved two Gaussian patches traversing the screen, with the observer required to fixate a central cross until they detected a luminance change in one of the patches, at which point a saccade was made to the brighter patch. In this experiment, however, the target changes speed some time after its luminance change. We use the subsequent relationship between saccade landing position and the time of speed change before saccade onset to examine target velocity integration.

Methods

Observers

Five observers were recruited from students and staff of the University of Bristol, UK (3 males and 2 females, age range 18–26, mean age 22). Two observers, including the first author, also took part in Experiment 1. All had self-reported normal or corrected-to-normal vision. Data were collected over three sessions, performed on different days. The study was approved by the local ethics committee.

Design and procedure

A similar set-up to Experiment 1 was used. In Experiment 2, static trials were removed, and in the movement trials, we introduced a noticeable step change in the velocity at a variable interval after the luminance change in the saccade target. In 50% of the trials, the patches would start moving at 18 deg/s and remain at this speed for the duration of the trial. In 25% of trials, the patches would step up from 18 to 30 deg/s after the luminance change occurred. In the remaining 25% of trials, the patches would step down in speed from 18 to 6 deg/s. A diagram outlining the procedure is shown in Figure 3. As with Experiment 1, observers were instructed to generate a saccade to the brighter patch as quickly and as accurately as possible. The same nonaging foreperiod for the luminance change occurred as for Experiment 1. A second nonaging foreperiod was used to determine the moment of the speed step, with a mean of 100 ms, and used a maximum cumulative probability of 95% to truncate the distribution.

Direction of motion was randomized from trial to trial such that in 50% of constant speed, step-up and step-down trials, the patches moved in a rightward direction across the screen and in a leftward direction in the other 50% of trials. The starting locations were determined such that the patches would be shown for at least 445 ms before the luminance change would occur. Observers completed 18 blocks of 96 trials in total.

Data analysis

As in Experiment 1, only data collected about the first saccade in each trial were considered for analysis. Trials in which the amplitude of the first saccade was less than 4 deg were rejected. Data from trials in which no saccade was made (either due to participants not detecting a target change or there being no target change), as well as data from trials in which the patches remained at constant speed were not included in further analysis. The primary analysis concerned the horizontal component of each saccade.

Results

By varying the interval between the luminance and velocity changes, and measuring the amount of error in the

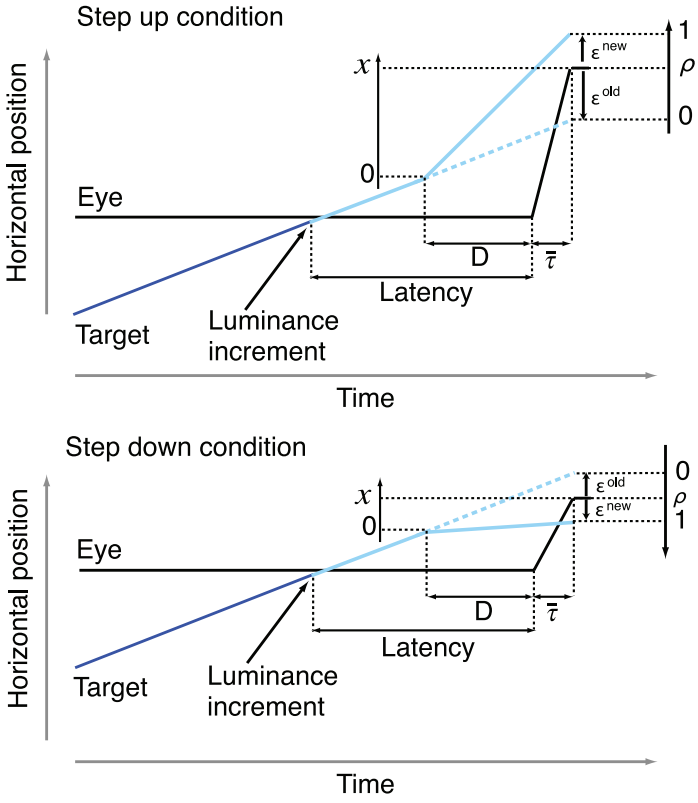

Figure 3. Time course of the target patch in a typical trial in Experiment 2. Note that the non-target patch follows the same time course but is not subject to the luminance increment. Target would begin moving at 18 deg/s. Following a luminance increment signaling which patch to make a saccade to, the target would then either (top) step up or (bottom) step down in speed to 30 deg/s or 6 deg/s, respectively. *D* denotes the time between velocity change and saccade onset. *x* denotes the component of saccade landing position from the velocity change to saccade end. ε^{old} denotes the difference between saccade landing position and the point where the target would have been if it had not changed speed, and ε^{new} denotes the difference between saccade landing position and the actual position of the target when the saccade landed. ρ denotes the relative weighting attributed to the new velocity.

subsequent saccade endpoint, we were able to gain insight into how much time is required to successfully integrate the motion signal arising from the second velocity into the saccade program. Figure 4A illustrates the error as a function of the time between the velocity change and saccade onset (termed *D*) for one observer. For clarity, *D* = 500 ms indicates that the velocity step occurred 500 ms before saccade onset.

For each saccade n, we can quantify to what extent the saccade was driven by the pre- and post-step velocities. We calculate two errors (see de Brouwer et al., 2002 for a similar approach): ε_n^{old} (the difference between saccade landing position and the point where the target would have been if it had not changed speed) and ε_n^{new} (the difference between saccade landing position and the actual position of the target when the saccade landed). The pre-step error can be calculated as

$$\varepsilon_n^{old} = x_n - v^{old}(D_n + \tau_n), \quad (2)$$

where x_n is the horizontal component of each observed saccade landing position from the point at which the velocity change occurred, τ_n is the saccadic duration, and v^{old} is the original target velocity. We assume that x_n is a

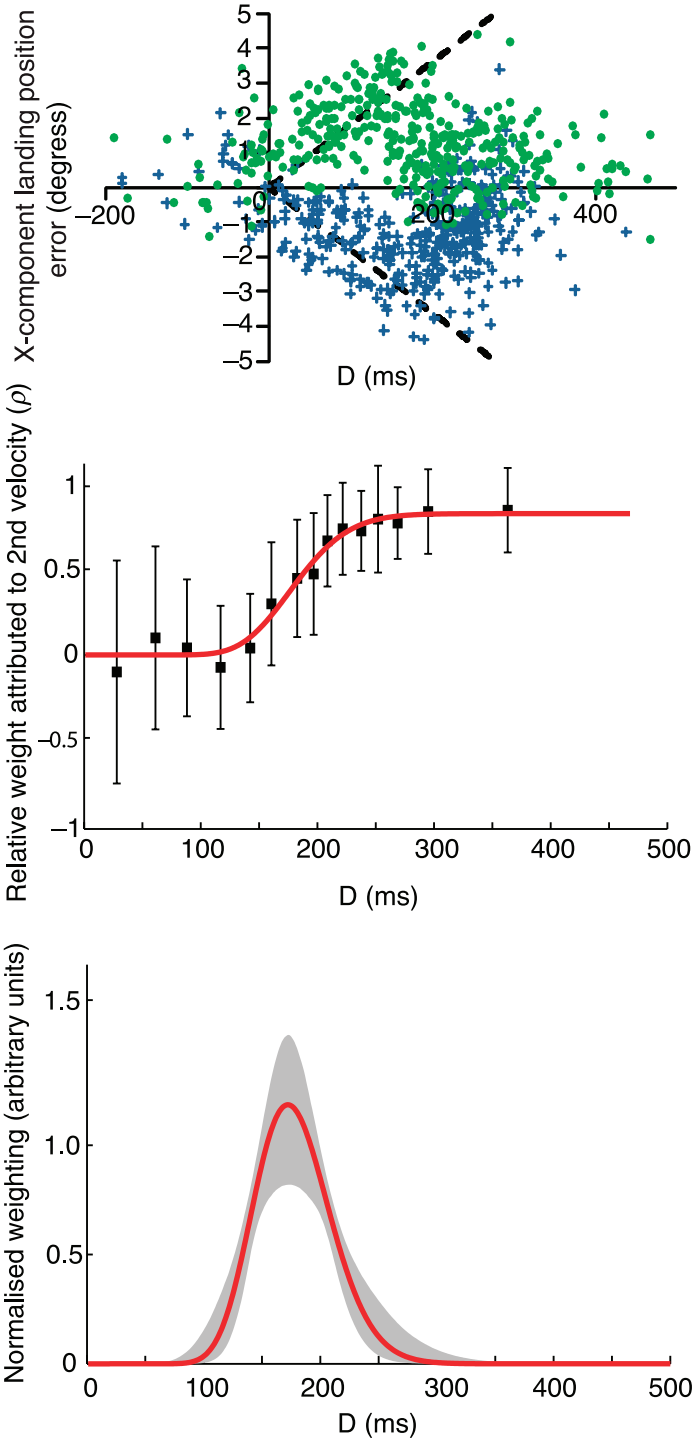

random sample from a Gaussian distribution with unknown mean ($\overline{x}_n$) and variance (σ_n^2). We also assume that τ_n is drawn from a Gaussian distribution with unknown mean ($\overline{\tau}_n$) and variance (ς_n^2). We make no initial assumptions about the manner in which the variance in τ_n and x_n varies as a function of D. In Figure 4A, the predicted landing position on the basis of the pre-step speed is shown by the dashed lines, which are based on the average saccade duration. These lines are shown for illustration purposes only; in actual fact, these functions will be slightly different from one trial to the next, depending on the saccade duration on that particular trial. However, these functions demonstrate the basic pattern of results: early in time the saccade landing positions follow the pre-step speed, but over time they fall more in line with the new velocity. In a similar manner to Equation 2, the post-step error can be expressed as

$$\varepsilon_n^{\text{new}} = x_n - v^{\text{new}}(D_n + \tau_n), \tag{3}$$

where v^{new} is the target velocity after the speed change.

The relative weight for saccade n attributed to the new velocity is

$$\rho_n = \frac{\varepsilon_n^{\text{old}}}{\varepsilon_n^{\text{old}} - \varepsilon_n^{\text{new}}}. \tag{4}$$

If the new velocity is not taken into account, then $\rho_n = 0$. On the other hand, if the new velocity is fully taken into account, then $\rho_n = 1$. If the process is conceived of as a step change (such as our velocity change) falling within a temporal integration kernel $f(t)$, then ρ_n is the proportion of the area under $f(t)$ that falls after the speed change. A plot of ρ_n at a range of values of D_n therefore gives us the integral of the temporal kernel. Figure 4B illustrates these weights in 15 roughly equal bins for illustration purposes only (the actual analyses always involved the data from individual trials). As expected, as D increases, the new velocity is increasingly taken into account. We now only need to fit some reasonable function given the form of the data, and then differentiate to obtain an estimate of the kernel.

To fit this function, we need to define the probability distribution from which ρ_n is a sample.[1] Following from Equation 2, we can express the probability distribution from which each $\varepsilon_n^{\text{old}}$ is drawn as

$$\varepsilon_n^{\text{old}} \sim \mathcal{N}\left[\overline{x}_n - v^{\text{old}}(D_n + \overline{\tau}_n), \sqrt{\sigma_n^2 + (v^{\text{old}}\varsigma_n)^2}\right]. \tag{5}$$

Substituting Equations 2 and 3 into the denominator (or scaling factor) of Equation 4 gives us

$$\begin{aligned}\varepsilon_n^{\text{old}} - \varepsilon_n^{\text{new}} &= (v^{\text{new}} - v^{\text{old}})(D_n + \tau_n)\\ &= v^{\Delta}(D_n + \tau_n),\end{aligned} \tag{6}$$

where ($v^{\text{new}} - v^{\text{old}}$) is a constant that we term v^{Δ}. Obviously, the variability in saccade landing position (σ_n) is factored out of the scaling factor because it affects $\varepsilon_n^{\text{new}}$ and $\varepsilon_n^{\text{old}}$ equally. The probability distribution of the scaling factor can therefore be expressed as

$$\varepsilon_n^{\text{old}} - \varepsilon_n^{\text{new}} \sim \mathcal{N}[v^{\Delta}(D_n + \overline{\tau}_n), v^{\Delta}\varsigma_n]. \tag{7}$$

Incorporating the probability distributions shown in Equations 5 and 7 into the ratio for the calculation of ρ_n (see Equation 4) gives us the following:

$$\rho_n \sim \frac{\mathcal{N}\left[\overline{x}_n - v^{\text{old}}(D_n + \overline{\tau}_n), \sqrt{\sigma_n^2 + (v^{\text{old}}\varsigma_n)^2}\right]}{\mathcal{N}\left[v^{\Delta}(D_n + \overline{\tau}_n), v^{\Delta}\varsigma_n\right]}, \; D_n > 0. \tag{8}$$

The ratio of normal distributions is not normally distributed (Geary, 1930), so we use the approach of Marsaglia (2006) to calculate the probability density function from the means and standard deviations of the numerator and denominator (see Marsaglia's page 8 and his associated C code, notably function $g(t)$ that we translated into Matlab).

Marsaglia's approach assumes that the denominator is always positive, which is a reasonable assumption in our case when v^{Δ} is positive (when the stimulus speeds up) but not when v^{Δ} is negative. With the latter, we simply multiply both numerator and denominator by −1. Note that the distribution is determined in part by the correlation between the two distributions, which, with some straightforward substitution and reworking of the standard equation for correlation, can be expressed as

$$r_n = \frac{v^{\text{old}}\varsigma_n}{\sqrt{\sigma_n^2 + (v^{\text{old}}\varsigma_n)^2}}. \tag{9}$$

Figure 4. (A) D (time between velocity change and saccade onset) vs. x-component error in saccade landing positions for observer 2. Blue crosses denote speed step-up trials; green circles denote speed step-down trials. Dashed lines indicate behavior expected had the saccadic system generated endpoints based solely on the pre-step velocity—note that the calculation of pre-step error includes saccade duration, as described in Equation 2. Expected behavior based on post-step velocity coincides with positive values lying on the x-axis (i.e., zero error). (B) These data were then collapsed and weighted according to the importance of the post-step speed, and a gamma curve fitted. Red solid line denotes the fit of a cumulative Gamma function. Error bars denote the standard deviation. (C) Red line denotes velocity integration kernel plot based on the data set for one observer. Shaded area indicates 95% confidence limits based on 10,000 bootstrap replications.

Equations 8 and 9 include a number of unknowns, specifically $\bar{x}_n$, σ_n, $\bar{\tau}_n$, and ς_n. Ultimately, it is the variation in mean landing position, $\bar{x}$, with D that is of critical interest. The remaining quantities are of less interest but do need to be specified. A complication is that any of these quantities may depend on D, which is implicit in the subscript n. Intuitively, it may seem that with increasing D the amplitudes of the movements are likely to increase: as time elapses since the speed change, the pattern will have moved further and so a larger movement is required in order to capture it. It is well established that endpoint variability tends to increase with movement size (Harris & Wolpert, 1998; van Beers, 2007, 2008). If it is indeed the case that saccade amplitude increases with D, then it would seem plausible that the endpoint variance should increase as well. Likewise, given the well-established relation between movement amplitude and duration (Carpenter, 1988) it follows that saccade duration should increase with D as well, with possible concomitant increase in duration variability. Indeed, there were several weak but significant correlations between D and saccade amplitude, as well as between D and saccade duration.

Therefore, we cannot assume that σ_n, ς_n, and $\bar{\tau}_n$ remain constant over D. Moreover, the dependence on D may vary across the step-up and step-down conditions, and we have no a priori expectations about the shape of these dependencies. To capture these relations parametrically would require the introduction of a number of additional free parameters. In order to keep our final model as parsimonious as possible, we chose to sample estimates of σ_n, ς_n, and $\bar{\tau}_n$ directly from the raw data for each observer. To capture any potential variation, we computed amplitude variance, mean duration, and duration variance for values of D ranging from 1 to 500 ms, using a Gaussian kernel.

The standard deviation (or bandwidth) of the kernel was set for each observer and step condition separately. The bandwidths were determined using a data-driven bandwidth selection technique (Bowman & Azzalini, 1997) and are shown across all combinations of observer and step condition in Table 1. This technique optimized the bandwidth of a Gaussian kernel density estimator used to approximate the probability function of D. Such techniques aim to find a bandwidth that does not unduly smooth the distribution, nor allow an undue amount of high-frequency noise into the distribution (Marron, 1988). We reasoned that as our variables of interest are sampled as a function of D, a bandwidth for the optimal sampling of D itself would also be optimal for the smoothing of σ_n, ς_n, and $\bar{\tau}_n$ as a function of D.

We then convolved our data consisting of the ordered set of τ_n and x_n with this Gaussian smoothing function, in order to produce an estimate of $\bar{\tau}_n$, ς_n, and σ_n for every value of D, in 1-ms increments. In other words, this allows us to calculate the variance in saccade landing position,

	Kernel widths (ms)	
Observer	Step up	Step down
1	27.8	26.9
2	25.8	32.2
3	36.3	42.9
4	32.3	29.3
5	36.8	34.7
Mean (*SD*)	31.9 (4.94)	33.2 (6.17)

Table 1. Gaussian smoothing function widths (in milliseconds) used for data smoothing for each observer and speed step condition.

the mean saccade duration, and its variability for every saccade n. Convolved values of $\bar{\tau}_n$ were given by

$$\bar{\tau}_n = \frac{\sum_{i=1}^{N} \omega_i \tau_i}{\sum_{i=1}^{N} \omega_i}, \tag{10}$$

where the vector of weights, ω, is the Gaussian smoothing function, sampled at 1-ms intervals and centered on the D value of the nth saccade. The resulting standard deviation in $\bar{\tau}_n$ (i.e., ς_n) is then given by

$$\varsigma_n = \sqrt{\frac{\sum_{i=1}^{N} \omega_i (\tau_i - \bar{\tau}_n)^2}{\sum_{i=1}^{N} \omega_i}}. \tag{11}$$

We apply the same process to calculate σ_n as a function of D. Figure 5 shows, for a single observer, the resulting smoothed estimates of $\bar{\tau}_n$, ς_n, and σ_n as a function of D. Incidentally, we replicated the fits reported below using a common function width of 30.0 ms across all observer/conditions (as this width lies close to the mean across observers), as well as with a range of widths from 20.0 ms to 45.0 ms. In all such circumstances, the replicated fits fell within the 95% confidence intervals reported below.

We now need to choose a functional form that describes the variation in $\bar{\rho}_n$ with D, where σ_n and ς_n jointly determine the scale of the residuals. In the absence of strong a priori expectations on the nature of the integration kernel, we fit ρ_n with a scaled cumulative Gamma distribution function, shown by the red line in Figure 4B (we did examine fits of a cumulative Gaussian curve, which is symmetrical, but found that the fit was inferior). Note that the function was fit using values of $D_n > 0$ only—as negative values of D_n correspond to instances in which the velocity change occurred after saccade onset, such trials cannot reasonably provide meaningful information about how the velocity change is incorporated into the programming of a saccade. The equation for the Gamma function used is

$$F(x|k,\theta) = \frac{a}{\theta^k \Gamma(k)} \int_0^x t^{k-1} e^{-\frac{t}{\theta}} dt, \tag{12}$$

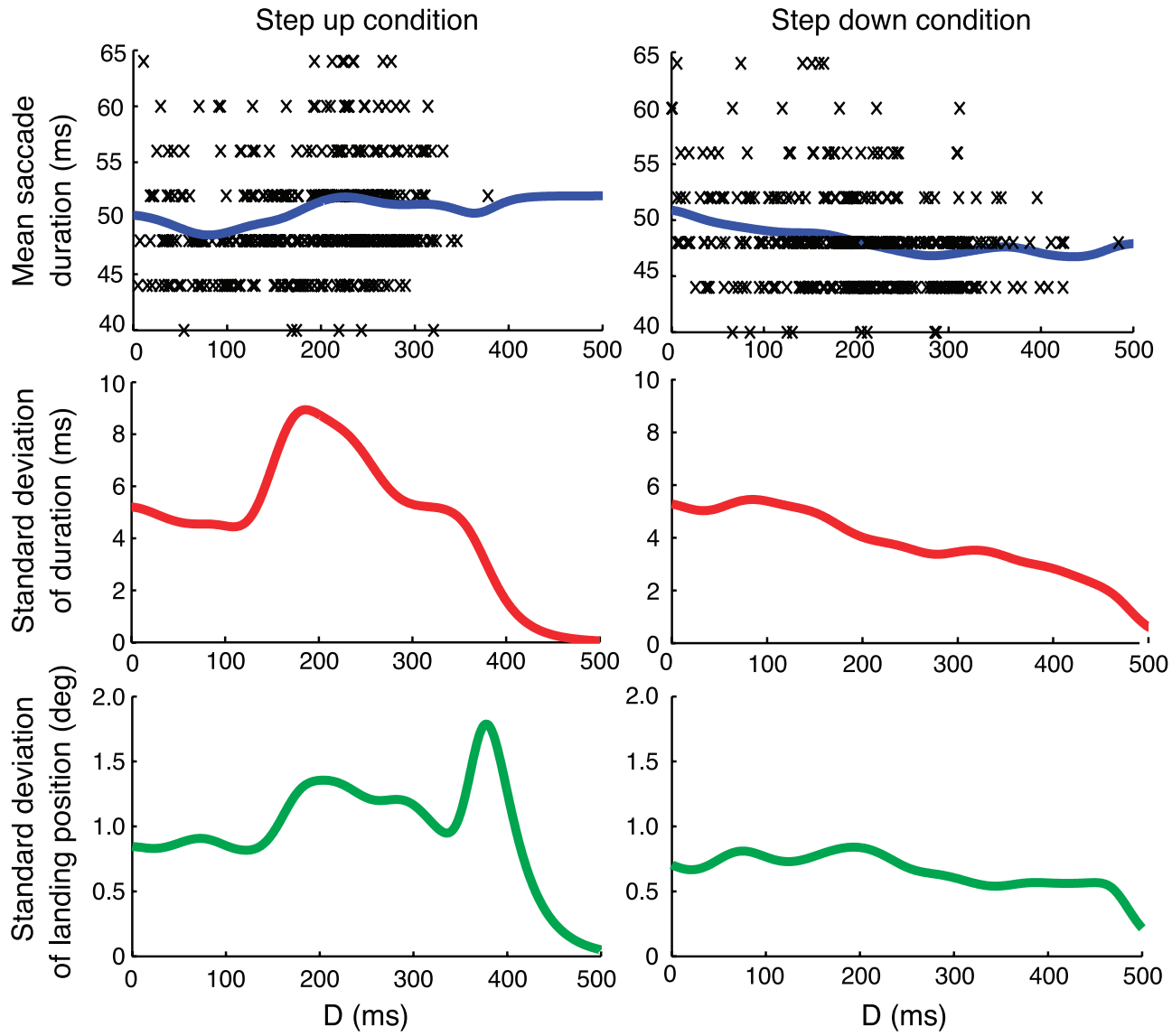

Figure 5. Plots of the Gaussian convolutions with the functions of *D* versus saccade duration and *D* versus landing position for a single observer for values of *D* ranging from 1 to 500 ms. Top and middle plots show the mean saccade duration ($\bar{\tau}$) and standard deviation of the duration (ς_n), respectively. Black dots in the top figure denote raw saccade durations. Bottom plot shows the standard deviation of the landing position (σ_n).

where k and θ are shape and scale parameters, respectively. The advantage of this functional form is that it can accommodate both symmetrical and asymmetrical kernels. To accommodate the data, we allow three parameters to vary: a (the upper bound of the curve fit − the lower bound was set to zero), k (shape), and θ (scale). To find a set of best-fitting parameters, we used the Simplex method (Nelder & Mead, 1965) to adjust the model parameters in order to maximize the likelihood of the observed values of ρ_n.

We initially calculated curve fits for the velocity increases and decreases separately; but within each observer, these gave very similar results. For the purposes of the final analysis, we therefore collapsed the data sets across these two conditions. The final step is then to take the derivative of the fitted scaled gamma distribution function (Figure 4C). The red line shows the kernel plot based on the data set for a single observer. The shaded region corresponds to the 95% confidence intervals. These were calculated by producing 10,000 bootstrap replications of the fitting parameters. Note that the bootstrap was conducted at the level of the raw data, such that in each iteration we calculated a new value of standard deviation of the smoothing function estimator, and therefore new values of σ_n, ς_n, and $\bar{\tau}_n$ for each observer/step condition. For values of D ranging from 1 to 500 in 1-ms increments, we calculated the weightings resulting from each bootstrap parameter set. For each sampled value of D, we then

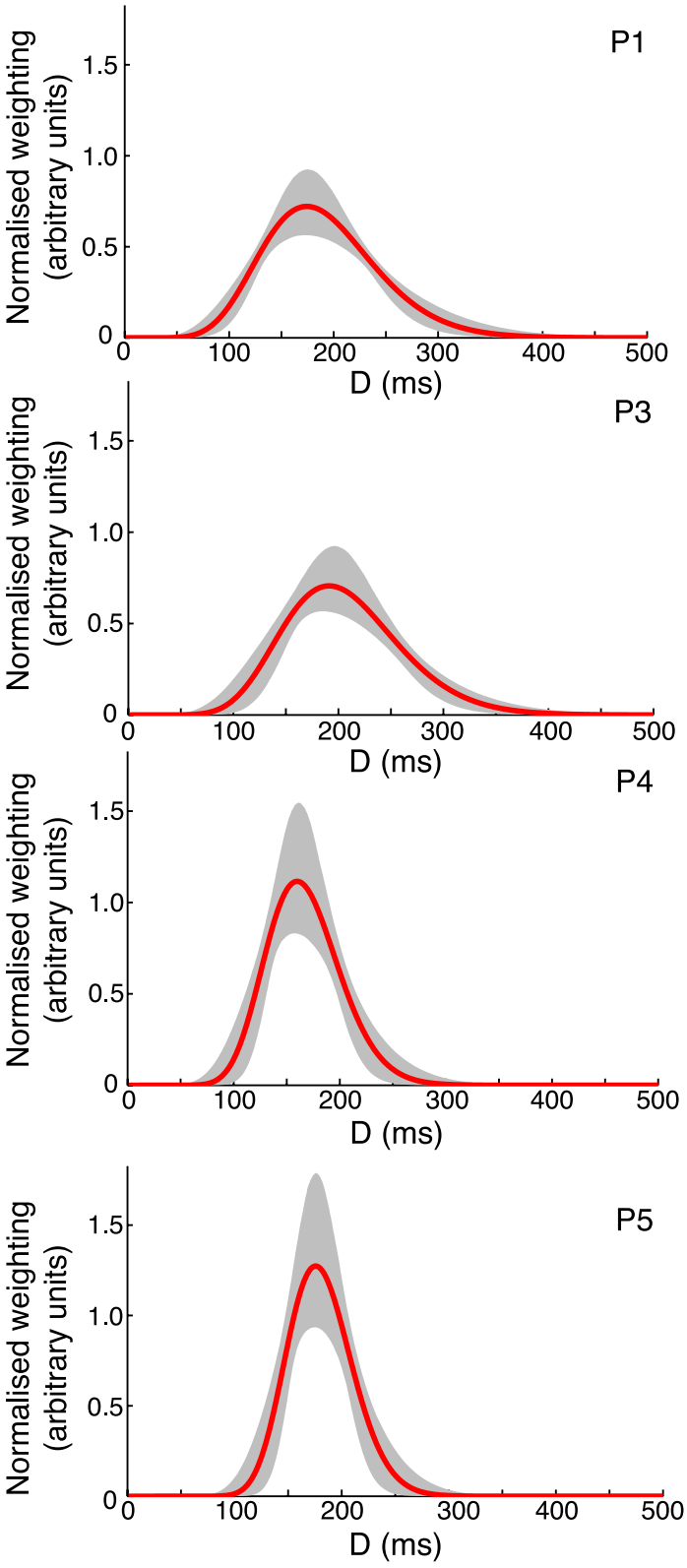

Figure 6. Velocity integration kernel plots for the remaining four observers (1, 3, 4, and 5). Red solid denotes the kernel plot based on each observer's data set. Shaded area indicates 95% confidence limits based on 10,000 bootstrap replications.

obtained the 95% confidence limits of the bootstrap weighting distributions at that point using the percentile method (Efron & Tibshirani, 1993).

Across all observers (see Figures 4C and 6), the kernel peaks suggest that the critical time for extracting information about the velocity signal occurs at a mean time of ~170 ms (*SEM* = 5.7 ms) before saccade onset. The mean full duration at half-maximum of the kernels is ~95 ms (*SEM* = 12.4 ms). After velocity estimation, there is a short gap of some 50–90 ms before saccade onset during which no new speed information is taken into account. Table 2 shows the resulting Gamma fit parameters for all five observers.

General discussion

Being able to rapidly and accurately move our eyes toward features or objects within our dynamic environment is an obvious prerequisite for rapid exploration of, and appropriate interaction with, our visual environment. The ability of the saccadic system to accurately intercept moving objects is clearly advantageous. It reduces the time needed for multiple catch-up eye movements, enabling faster responses to potentially important visual events. However, accurate fixation of moving objects requires the system to predict where the target will be when the movement is complete (Kerzel & Gegenfurtner, 2003). To get this prediction right, the system would need to compensate for the neural delays that intervene between movement planning and execution. The aim of this study was to identify how such compensation depends on the velocity of the moving target.

First of all, it was necessary to show that target velocity is indeed taken into account in the prediction process. The results from our first experiment provide clear evidence for a velocity-dependent contribution, which is consistent with previous behavioral data from non-human primates (Barborica & Ferrera, 2003; Cassanello et al., 2008; Eggert et al., 2005) as well as observations on catch-up saccades during smooth pursuit in humans (de Brouwer et al., 2002).

Having demonstrated a role for target velocity, we proceeded to identify the temporal window over which the velocity estimate was extracted. Our second experiment shows that, as the visual temporal integration window crosses a velocity change, the saccadic system produces a landing point based on a weighted average of the two velocities by increasingly giving more importance to the post-step velocity. In other words, the saccadic system is able to apply a moving integration window to the velocity signal in a manner that constantly updates the averaged velocity and uses this to determine the likely future location of an object in order to produce viable saccade endpoints. Whether a similar visual mechanism is involved in the

	Fit parameters			95% Confidence intervals		
Observer	*a*	*k*	θ	*a*	*k*	θ
1	0.94	11.92	15.96	0.90	7.67	9.62
				1.00	19.26	25.92
2	0.80	29.50	6.04	0.77	14.84	3.72
				0.87	47.55	12.36
3	0.84	13.55	15.23	0.81	8.61	8.55
				0.88	24.07	24.04
4	0.81	22.76	7.34	0.77	12.82	3.68
				0.85	44.98	13.24
5	0.84	35.20	5.14	0.79	19.41	2.50
				0.89	72.02	9.44

Table 2. Gamma fit parameters *a* (upper bound), *k* (shape), and θ (scale) and associated confidence intervals for all five observers. Confidence intervals were calculated based on 10,000 bootstrap replications.

generation of accurate catch-up saccades during smooth pursuit is an open question. However, given the considerable neural and functional overlap between the pursuit and saccadic systems (e.g., Blohm, Optican, & Lefèvre, 2006; Krauzlis & Stone, 1999), it would seem plausible to suggest that it is.

Recently, optimal linear filters have been described linking perturbations in target velocity and eye velocity during pursuit maintenance (Tavassoli & Ringach, 2009). Tavassoli and Ringach used a white noise analysis, whereby eye velocity was measured during pursuit of a Gabor patch that moved at constant speed with Gaussian white noise added to it. From this, they derived the optimal linear filter linking fluctuations in target velocity to those elicited in eye velocity. These filters showed times to peak ranging from 103 ms to 126 ms (our peak times did not occur before at least approximately 165 ms), and effective widths on the order of 45 ms, or about half the width of our integration kernels. They also showed pursuit delays ranging between 61 ms and 73 ms, which are comparable to our saccadic dead time estimates. Tavassoli and Ringach note that effective widths of around 45 ms are comparable to those found for individual direction-selective cells found in V1 in non-human primates and MT (e.g., Bair & Movshon, 2004).

There are a number of reasons why the combination of differences (in times to peak and widths) and similarities (dead time) noted above might occur. Conceivably, our integration kernels may be artificially stretched or squashed due to the fact that they are limited by saccade latency. However, our observed values of *D* are simply a sampling of the temporal kernel. If they fail to adequately sample that kernel, then this will simply lead to a lack of adequate constraint in our kernel estimates. It is more likely that the differences in findings reflect the differences in task demands. Tavassoli and Ringach were concerned with pursuit maintenance, which is generally thought to involve the modulation of a continuous movement based on feedback about performance quality and target velocity that minimizes retinal slip (Lencer & Trillenberg, 2008; Lisberger, Morris, & Tychsen, 1987). The feedback involves a combination of retinal (i.e., image displacement) and extra-retinal (i.e., efference copy and proprioception from the ocular muscles) sources of information (e.g., Krauzlis & Lisberger, 1994; Lisberger, Evinger, Johanson, & Fuchs, 1981).

Our task involved a primary orienting saccade in which the eyes break from fixation in order to intercept a moving target. Critically, whereas during pursuit maintenance, the intended target of interest is clearly known, our task was specifically designed so that the location of the desired saccade target was unpredictable. As such, only retinal information is available to the saccadic system, with the added requirement to select a target over a competing non-target. It is possible that during pursuit maintenance, the combination of retinal and extra-retinal signals, in conjunction with the absence of the need to select a target, enables the pursuit system to respond to changes in the visual input with greater temporal precision than that found for our primary orienting saccades.

More generally, suggestions regarding the integration of velocity information into an appropriate response have been made in the motion integration literature: when presented with a stimulus containing a number of different spatially interspersed speeds, the visual system averages them together (Watamaniuk & Duchon, 1992) and it has recently been suggested that we temporally integrate local motion when making speed estimates from complex velocity fields (Benton & Curran, 2009). At the point in time when a saccade is imminent, a saccade landing position is generated from a signal that combines the averaged velocity signal with information about the target position taken prior to the saccadic dead time.

Brain area MT is widely believed to be important for motion integration (Born & Bradley, 2005). As reviewed earlier, lesions to MT abolished the ability to generate accurate saccades to moving targets (Newsome et al., 1985), and it has been shown that MT neurons are sensitive not only to motion direction but also to object speed (Perrone & Thiele, 2001). In addition, MT projects to eye movement-related structures such as the superior colliculus (SC; Ungerleider, Desimone, Galkin, & Mishkin, 1984) and FEF (Tian & Lynch, 1996), which—in turn—are reciprocally connected. It also projects to the cerebellum (CB) via the pontine nuclei (Maunsell & Essen, 1983). The SC and CB also receive projections from lateral intraparietal cortex and FEF neurons (Optican & Quaia, 2002; Quaia, Lefèvre, & Optican, 1999).

Motor maps such as those found in SC and FEF were traditionally thought of as encoding the desired gaze vector (e.g., Robinson, 1972; Stein, Goldberg, & Clamann, 1976; see also Klier, Wang, & Crawford, 2001). For saccades to a moving target then, the population code on such motor maps would need to reflect a combination of

the sampled position error, shifted by the velocity-dependent offset. Such signals have, to our knowledge, not been observed in any of these eye movement-related structures (e.g., Optican, 2005). An alternative view is suggested by Optican and Quaia (2002). For saccades to moving targets, the collicular site activated encodes the initial target location (note, not the desired movement), which is subsequently fed into a downstream feedback circuit involving the brainstem and CB (Optican & Quaia, 2002; Robinson, 1972). Because the CB has access to motion-related signals emanating from MT, we speculate that this may be the level in the system at which the appropriate offset is accomplished.

Finally, the fact that the post-step velocity can have an influence on saccade endpoints as little as 50–90 ms before saccade onset shows how late in the process eye movements can be modified based on novel incoming information. Comparable estimates of dead time can be found for saccades, for example in double-step experiments (e.g., Becker & Jürgens, 1979; Gellman & Carl, 1991b; Ludwig, Mildinhall, & Gilchrist, 2007) and in a temporal noise classification study (e.g., Caspi et al., 2004). Similarly with pursuit eye movements, studies have shown, in "gap paradigm" experiments in which visual information is modified as little as 30–100 ms before pursuit onset, that significant decreases in latency can be found (Krauzlis & Miles, 1996a, 1996b).

In conclusion, the present study confirms our assumption that information about target velocity is available to the saccadic system during the saccade planning process. We then characterize the mechanism by which this occurs by measuring the temporal window that is used to extract this information. We have demonstrated that the saccadic system, rather than relying on a constant offset applied to retinal position error, takes a temporally blurred snapshot of target velocity in the latency period preceding saccade generation. This information is used to generate a dynamically updated prediction of the target's likely future location, which enables the programming of an accurate motor response to a moving target.

Acknowledgments

This work was supported by the Biotechnology and Biological Sciences Research Council. CL is supported by an Advanced Research Fellowship from the Engineering and Physical Sciences Research Council (EP/E054323/1). The authors would like to thank two anonymous reviewers for helpful suggestions.

Commercial relationships: none.
Corresponding author: Peter J. Etchells.
Email: peter.etchells@bristol.ac.uk.
Address: Department of Experimental Psychology, University of Bristol, Bristol, UK.

Footnote

[1]Specifying the probability distribution is necessary for maximum-likelihood estimation of the kernel parameters. Fits using least squares or least absolute residuals do not require explicit identification of this probability distribution, as a function of D. Indeed, fits using these simpler methods result in similar parameter estimates as the ones reported in Table 2. We specify a more complete model here, because we feel it is important to make explicit what sources of variance contribute to the variation in ρ_n.

References

Aslin, R. N., & Shea, S. L. (1987). The amplitude and angle of saccades to double-step target displacements. *Vision Research, 27,* 1925–1942.

Bahill, A. T., & Stark, L. (1975). Neurological control of horizontal and vertical components of oblique saccadic eye movements. *Mathematical Biosciences, 27,* 287–298.

Bair, W., & Movshon, J. A. (2004). Adaptive temporal integration of motion in direction-selective neurons in macaque visual cortex. *Journal of Neuroscience, 24,* 7305–7323.

Barborica, A., & Ferrera, V. P. (2003). Estimating invisible target speed from neuronal activity in monkey frontal eye field. *Nature Neuroscience, 6,* 66–74.

Barborica, A., & Ferrera, V. P. (2004). Modification of saccades evoked by stimulation of frontal eye field during invisible target tracking. *Journal of Neuroscience, 24,* 3260–3267.

Becker, W. (1989). Metrics. In R. H. Wurtz & M. E. Goldberg (Eds.), *The neurobiology of saccadic eye movements* (pp. 13–67). Amsterdam, The Netherlands: Elsevier.

Becker, W., & Jürgens, R. (1979). An analysis of the saccadic system by means of double-step stimuli. *Vision Research, 19,* 967–983.

Benton, C. P., & Curran, W. (2009). The dependence of perceived speed upon signal intensity. *Vision Research, 49,* 284–286.

Blohm, G., Optican, L. M., & Lefèvre, P. (2006). A model that integrates eye velocity commands to keep track of smooth eye displacements. *Journal of Computational Neuroscience, 21,* 51–70.

Born, R. T., & Bradley, D. C. (2005). Structure and function of visual area MT. *Annual Review of Neuroscience, 28,* 157–189.

Bowman, A. W., & Azzalini, A. (1997). *Applied smoothing techniques for data analysis*. Oxford, UK: Oxford University Press.

Brainard, D. H. (1997). The psychophysics toolbox. *Spatial Vision, 10,* 433–436.

Carpenter, R. H. S. (1988). *Movements of the eyes* (2nd ed.). London: Pion.

Caspi, A., Beutters, B. R., & Eckstein, M. P. (2004). The time course of visual information accrual guiding eye movement decisions. *Proceedings of the National Academy of Sciences of the United States of America, 101,* 13086–13090.

Cassanello, C. R., Nihalani, A. T., & Ferrera, V. P. (2008). Neuronal responses to moving targets in monkey frontal eye fields. *Journal of Neurophysiology, 100,* 1544–1556.

Cornelissen, F. W., Peters, E. M., & Palmer, J. (2002). The eyelink toolbox: Eye tracking with MATLAB and the psychophysics toolbox. *Behaviour Research Methods, Instruments & Computers, 34,* 613–617.

de Brouwer, S., Missal, M., Barnes, G., & Lefèvre, P. (2002). Quantitative analysis of catch-up saccades during sustained pursuit. *Journal of Neurophysiology, 87,* 1772–1780.

Efron, B., & Tibshirani, R. J. (1993). *An introduction to the bootstrap. Monographs on statistics and applied probability*. Boca Raton, FL: Chapman & Hall/CRC.

Eggert, T., Guan, Y., Bayer, O., & Buttner, U. (2005). Saccades to moving targets. *Annals of the New York Academy of Sciences, 1039,* 149–159.

Findlay, J. M., & Harris, L. R. (1984). Small saccades to double-stepped targets moving in two dimensions. In A. G. Gale & F. Johnson (Eds.), *Theoretical and applied aspects of eye movement research* (pp. 71–78). Amsterdam, The Netherlands: Elsevier.

Geary, R. C. (1930). The frequency distribution of the quotient of two normal variates. *Journal of the Royal Statistical Society, 90,* 442–446.

Gellman, R. S., & Carl, J. R. (1991a). Early responses to double-step targets are independent of step amplitude. *Experimental Brain Research, 87,* 433–437.

Gellman, R. S., & Carl, J. R. (1991b). Motion processing for saccadic eye movements in humans. *Experimental Brain Research, 84,* 660–667.

Harris, C. M. (1994). Does saccadic undershoot minimize saccadic flight-time? A Monte-Carlo study. *Vision Research, 35,* 691–701.

Harris, C. M., & Wolpert, D. M. (1998). Signal-dependent noise determines motor planning. *Nature, 394,* 780–784.

Heywood, S., & Churcher, J. (1981). Saccades to step-ramp stimuli. *Vision Research, 21,* 479–490.

Ilg, U. J., & Thier, P. (2003). Visual tracking neurons in primate area MST are activated by smooth-pursuit eye movements of an "imaginary" target. *Journal of Neurophysiology, 90,* 1489–1502.

Keller, E., & Johnsen, S.D. (1990). Velocity prediction in corrective saccades during smooth-pursuit eye movements in monkey. *Experimental Brain Research, 80,* 525–531.

Kerzel, D., & Gegenfurtner, K. R. (2003). Neuronal processing delays are compensated in the sensorimotor branch of the visual system. *Current Biology, 13,* 1975–1978.

Kim, C. E., Thaker, G. K., Rosse, D. E., & Medoff, D. (1997). Accuracies to saccades to moving targets during pursuit initiation and maintenance. *Experimental Brain Research, 113,* 371–377.

Klier, E. M., Wang, H., & Crawford, J. D. (2001). The superior colliculus encodes gaze commands in retinal coordinates. *Nature Neuroscience, 4,* 627–632.

Krauzlis, R. J. (2004). Recasting the smooth pursuit eye movement system. *Journal of Neurophysiology, 91,* 591–603.

Krauzlis, R. J., & Lisberger, S. G. (1994). Temporal properties of visual motion signals for the initiation of smooth pursuit eye movements in monkeys. *Journal of Neurophysiology, 72,* 150–162.

Krauzlis, R. J., & Miles, F. A. (1996a). Initiation of saccades during fixation or pursuit: Evidence in humans for a single mechanism. *Journal of Neurophysiology, 76,* 4175–4179.

Krauzlis, R. J., & Miles, F. A. (1996b). Release of fixation for pursuit and saccades in humans: Evidence for shared inputs acting on different neural substrates. *Journal of Neurophysiology, 76,* 2822–2832.

Krauzlis, R. J., & Stone, L. S. (1999). Tracking with the mind's eye. *Trends in Neuroscience, 22,* 544–550.

Lencer, R., & Trillenberg, P. (2008). Neurophysiology and neuroanatomy of smooth pursuit in humans. *Brain and Cognition, 68,* 219–228.

Lisberger, S. G., Evinger, C., Johanson, G. W., & Fuchs, A. F. (1981). Relationship between eye acceleration and retinal image velocity during foveal smooth pursuit in man and monkey. *Journal of Neurophysiology, 46,* 229–249.

Lisberger, S. G., Morris, E. J., & Tychsen, L. (1987). Visual motion processing and sensory motor integration for smooth pursuit eye movements. *Annual Review of Neuroscience, 10,* 97–129.

Liston, D., & Krauzlis, R. J. (2005). Shared decision signal explains performance and timing of pursuit and saccadic eye movements. *Journal of Vision, 5*(9):3, 678–689, http://www.journalofvision.org/content/5/9/3, doi:10.1167/5.9.3. [PubMed] [Article]

Ludwig, C. J. H., Mildinhall, J. W., & Gilchrist, I. D. (2007). A population coding account for systematic variation in saccadic dead time. *Journal of Neurophysiology, 97,* 795–805.

Marron, J. S. (1988). Automatic smoothing parameter selection: A survey. *Empirical Economics, 13,* 187–208.

Marsaglia, G. (2006). Ratios of normal variables. *Journal of Statistical Software, 16,* 1–10.

Maunsell, J. H. R., & Essen, D. C. V. (1983). The connections of the middle temporal visual area (MT) and their relationship to a cortical hierarchy in the macaque monkey. *Journal of Neuroscience, 3,* 2563–2586.

Nelder, J. A., & Mead, R. (1965). A simplex-method for function minimization. *Computer Journal, 7,* 308–313.

Newsome, W. T., Wurtz, R. H., Dursteler, M. R., & Mikami, A. (1985). Deficits in visual-motion processing following ibotenic acid lesions of the middle temporal visual area of the macaque monkey. *Journal of Neuroscience, 5,* 825–840.

Optican, L. M. (2005). Sensorimotor transformation for visually guided saccades. *Annals of the New York Academy of Sciences, 1039,* 132–148.

Optican, L. M., & Quaia, C. (2002). Distributed model of collicular and cerebellar function during saccades. *Annals of the New York Academy of Sciences, 956,* 164–177.

Orban de Xivry, J. J., & Lefèvre, P. (2007). Saccades and pursuit: Two outcomes of a single sensorimotor process. *The Journal of Physiology, 584,* 11–23.

Oswal, A., Ogden, M., & Carpenter, R. H. S. (2007). The time course of stimulus expectation in a saccadic decision task. *Journal of Neurophysiology, 97,* 2722–2730.

Perrone, J. A., & Thiele, A. (2001). Speed skills: Measuring the visual speed analyzing properties of primate MT neurons. *Nature Neuroscience, 4,* 526–532.

Quaia, C., Lefèvre, P., & Optican, L. M. (1999). Model of the control of saccades by superior colliculus and cerebellum. *Journal of Neurophysiology, 82,* 999–1018.

Robinson, D. A. (1972). Eye movements evoked by collicular stimulation in the alert monkey. *Vision Research, 12,* 1795–1808.

Robinson, D. A. (1973). Models of the saccadic eye movement control system. *Kybernetic, 14,* 71–83.

Ron, S., Vieville, T., & Droulez, J. (1989). Target velocity based prediction in saccadic vector programming. *Vision Research, 29,* 1103–1114.

Schall, J. D. (1999). Weighing the evidence: How the brain makes a decision. *Nature Neuroscience, 2,* 108–109.

Schiller, P. H., & Tehovnik, E. J. (2005). Neural mechanisms underlying target selection with saccadic eye movements. *Progress in Brain Research, 149,* 157–171.

Seijas, O., Gómez de Liaño, P., Gómez de Liaño, R., Roberts, C. J., Piedrahita, E., & Diaz, E. (2007). Ocular dominance diagnosis and its influence in monovision. *American Journal of Ophthalmology, 144,* 209–216.

Stampe, D. M. (1993). Heuristic filtering and reliable calibration methods for video-based pupil-tracking systems. *Behavior Research Methods, Instruments & Computers, 25,* 137–142.

Stein, B. E., Goldberg, S. J., & Clamann, H. P. (1976). The control of eye movements by the superior colliculus in the alert cat. *Brain Research, 118,* 469–474.

Tavassoli, A., & Ringach, D. L. (2009). Dynamics of smooth pursuit maintenance. *Journal of Neurophysiology, 102,* 110–118.

Tian, J. R., & Lynch, J. C. (1996). Corticocortical input to the smooth and saccadic eye movement subregions of the frontal eye field in Cebus monkeys. *Journal of Neurophysiology, 76,* 2754–2771.

Ungerleider, L. G., Desimone, R., Galkin, T. W., & Mishkin, M. (1984). Subcortical projections of area MT in the macaque. *Journal of Computational Neurology, 223,* 368–386.

van Beers, R. J. (2007). The sources of variability in saccadic eye movements. *Journal of Neuroscience, 27,* 8757–8770.

van Beers, R. J. (2008). Saccadic eye movements minimise the consequences of motor noise. *PloS ONE, 3,* e2070.

Watamaniuk, S. N. J., & Duchon, A. (1992). The human visual-system averages speed information. *Vision Research, 32,* 931–941.